PNAS RESEARCH ARTICLE | ECOLOGY
BIOPHYSICS AND COMPUTATIONAL BIOLOGY OPEN ACCESS

Dynamic coexistence driven by physiological transitions in microbial communities

Avaneesh V. Narla[a], Terence Hwa[a,1], and Arvind Murugan[b,1]

Affiliations are included on p. 11.

Contributed by Terence Hwa; received March 19, 2024; accepted March 17, 2025; reviewed by Jacopo Grilli and Sergei Maslov

Microbial ecosystems are commonly modeled by fixed interactions between species in steady exponential growth states. However, microbes in exponential growth often modify their environments so strongly that they are forced out of the growth state into stressed, nongrowing states. Such dynamics are typical of ecological succession in nature and serial-dilution cycles in the laboratory. Here, we introduce a phenomenological model, the Community State Model, to gain insight into the dynamic coexistence of microbes due to changes in their physiological states during cyclic succession. Our model specifies the growth preference of each species along a global ecological coordinate, taken to be the biomass density of the community, but is otherwise agnostic to specific interactions (e.g., nutrient starvation, stress, aggregation), in order to focus on self-consistency conditions on combinations of physiological states, "community states," in a stable ecosystem. We identify three key features of such dynamical communities that contrast starkly with steady-state communities: enhanced community stability through staggered dominance of different species in different community states, increased tolerance of community diversity to fast growing species dominating distinct community states, and increased requirement of growth dominance by late-growing species. These features, derived explicitly for simplified models, are proposed here as principles aiding the understanding of complex dynamical communities. Our model shifts the focus of ecosystem dynamics from bottom–up studies based on fixed, idealized interspecies interaction to top–down studies based on accessible macroscopic observables such as growth rates and total biomass density, enabling quantitative examination of community-wide characteristics.

microbial ecology | bacterial physiology | community assembly | ecological succession

Significance

Microbial ecosystems in nature exhibit dynamic lifecycles, cycling through distinct physiological states for the microbes as they switch between active growth, stressed states, and dormancy. Constructing mechanistic bottom–up models that incorporate these changes is challenging because experimental data do not sufficiently constrain the many parameters. Consequently, current models typically assume constant exponential growth and fixed pairwise interactions, missing the critical link between physiology and ecology. Instead, we present a phenomenological model, the Community State Model, that emphasizes the changing physiological state of community members rather than individual interactions. Our model provides testable predictions about the emergent structure of microbial communities with dynamic lifecycles.

Microbial communities in natural environments are often highly dynamic, with both endogenous and exogenous changes (1–7). Exogenous changes include periodic replenishment of resources [e.g., the mammalian gut (8) and the ocean (9)], or resetting of other environmental factors with periods of growth between these perturbations (10, 11). Even laboratory experiments (12–14) on microbial ecosystems frequently adopt serial dilution cycles with dynamic environments. In the case of endogenous changes, recent studies have found that stable microbial communities do not settle simply into a fixed state, but are instead driven through dynamic phases involving complex changes in the environment such as depletion of oxygen and build-up of toxic waste (15–17). These changes, in turn, alter the physiological states of the microbes in the community, slowing down or even halting their growth. Changes in physiological states are often reflected in changes in an organism's metabolic uptake and secretion profiles and can induce more complex behaviors such as aggregation, motility, toxin secretion, and contact-dependent inhibition (18–21).

These observations have been interpreted using bottom–up models from theoretical ecology (22, 23), which attempt to account for ecosystem assembly and stability in terms of mechanistic effects such as resource competition arising from hardwired nutrient preferences and gene expression responses (12, 13, 24). However, the mechanistic effects invoked are mostly taken to be driven by changes in the environment, e.g., nutrient concentrations, but not the state of the cell (22, 25–28). This assumption is practical, as most mechanistic effects, to the extent they have been characterized quantitatively, have been done for cells in exponential growth (11, 29–31).

This gulf between empirical observations and theoretical models raises questions about the consequences of dynamic physiological state changes in shaping complex communities (32). One possibility is that physiological state changes are merely details,

Author contributions: A.V.N., T.H., and A.M. designed research; performed research; analyzed data; and wrote the paper.

Reviewers: J.G., Abdus Salam International Centre for Theoretical Physics; and S.M., University of Illinois at Urbana Champaign.

The authors declare no competing interest.

[1]To whom correspondence may be addressed. Email: thwa@ucsd.edu or amurugan@uchicago.edu.

This article contains supporting information online at https://www.pnas.org/lookup/suppl/doi:10.1073/pnas.2405527122/-/DCSupplemental.

Published April 17, 2025.

not essential for understanding factors that enable community assembly. From this perspective, nothing is lost by coarse-graining over dynamics and modeling communities as if they are in steady state. We would expect the community's diversity and structure to remain similar, regardless of whether microbes are in a stable growth phase (e.g., exponential growth) or whether interactions like metabolite secretion and uptake occur in a temporally staged manner.

Another possibility is that physiological state changes create dynamic niches that support complex communities. Since microbes have a plethora of nongrowing states, this scenario could significantly expand the ways of generating niches beyond well-studied cases such as growth on distinct metabolites (27), partitioning of real space (33), and division of externally dictated temporal epochs (e.g., periods in diel or annual cycles) (34). Such self-generated dynamic niches, if they exist, might have signatures that are observable in microbial communities.

It is experimentally and theoretically challenging to understand the effect of physiological state changes using the canonical bottom–up theoretical frameworks, such as the generalized Lotka–Volterra (gLV) or Consumer–Resource (CR) models, since these models typically characterize organisms and their interactions with fixed parameters. In these models, community dynamics only involves changes in species abundances and nutrient concentrations, with all interaction parameters taken to be fixed in time, reflecting the underlying assumption that each organism is in a fixed physiological state (e.g., exponential growth). Hence, in bottom–up models, each physiological state would minimally involve a different set of uptake and excretion parameters; a given species would effectively be modeled as multiple species over time. Thus, bottom–up models of dynamic communities require extensive characterization and unconstrained assumptions on specific details about what different cells do in different conditions.

As a step toward quantitatively modeling communities of species that undergo changes in physiological states, we introduce a minimal top–down phenomenological framework, the Community State (CS) Model. Our model is phenomenological at the level of species density: the physiological state and thus the growth rate of each species in a community is assumed to depend on a single dynamical coordinate. This coordinate is taken here to be the community biomass, and as a result, community states are defined by biomass density intervals. Such a model can be solved explicitly (numerically and in simple cases analytically) to yield the temporal organization of community dynamics at a quantitative level.

Analysis of the CS Model points to sequential dynamics as a strategy to form a stable community involving multiple species (35), a scenario that is underexplored in the current literature. In this simple model, each species grows rapidly in one (or a few) community states, defined over specific intervals of biomass density, with little growth in other intervals. This strategy is a distinct alternative to the cogrowth strategy based on steady-state models with fixed physiological states, where many species grow on resource niches simultaneously.

For this sequential growth strategy, our model reveals a number of interesting features of community dynamics. We find a) enhanced community stability by coordinating staggered dominance of different species in different community states, b) tolerance of community diversity to fast-growing species if such growth is limited to specific community states, and c) a requirement of increased growth dominance for late-growing species. These features counteract the dominant notions regarding species competition derived from steady-state systems, and serve as principles to guide the understanding of complex dynamical ecosystems.

Results

Case Study of Community Dynamics During Serial-Dilution Cycles. The model of microbial community dynamics developed here is inspired by a recent study of a seemingly simple cross-feeding system subjected to repeated serial-dilution cycles (16): two species of marine bacteria, *Vibrio* sp. 1A01 and *Neptunomonas* sp. 3B05, isolated from a chitin-degrading coastal community (36), were grown on N-acetyl glucosamine (GlcNAc) as the sole carbon and nitrogen sources in batch culture. 1A01 consumes GlcNAc and excretes acetate and ammonium, while 3B05, which does not consume GlcNAc, can grow on the acetate and ammonium excreted by 1A01 (Fig. 1*A*). Because 1A01 grows on GlcNAc faster than 3B05 grows on acetate, acetate inevitably accumulates in the medium, becoming toxic when reaching the buffer capacity of the medium [which is low for seawater (37)]. In canonical syntrophy, toxicity would slow down the toxin-excreting species more than the toxin-clearing species, resulting in a stable state where both species grow exponentially (38). This is not the case for the 1A01–3B05 coculture: acetate accumulation in the environment slows down the growth of 3B05, the acetate-consumer, more than that of 1A01, the acetate excretor. Thus acetate is expected to accumulate, eventually arresting the growth of the coculture. Since 1A01 grows faster and is inhibited later, its gain should exceed that of 3B05 after a cycle of growth, so that after a number of growth–dilution cycles, 1A01 should dominate and 3B05 be purged. This indeed happens for the 6-h growth–dilution cycles (*Left* panel, Fig. 1*B*). Yet when this system was subjected to 24-h cycles, the two species managed to settle down to a "stable cycle" after just a few transient cycles, with comparable abundances and no acetate in the medium, based on measurements at the end of each 24-h cycle.

Detailed analysis of the two-species dynamics revealed that stability was achieved through a series of physiological transitions during the 24-h growth period (*Right* panel, Fig. 1*B*). The community went through a sequence of six states, ⓪ to ⑤, each corresponding to a distinct combination of the physiological states of the individual species as listed in Fig. 1*C*. The dynamics of system is illustrated as a trajectory in the space of the concentrations of the three metabolites (Fig. 1*D*) or as plots of the growth rates of the two species over time (Fig. 1*E*): the first state ⓪ after dilution and nutrient replenishment is one where 1A01 adapts from the previous cycle without growth, but nevertheless converts small amounts of GlcNAc into acetate, enabling some slow growth of 3B05. This state occupies ∼1/3 of the duration of the growth–dilution cycle (Fig. 1*E*) but results little biomass changes (*Right* panel, Fig. 1*B*). The next state ① is dominated by the rapid growth of 1A01, which consumes large amounts of GlcNAc and excretes nearly equal molar of acetate, fueling the (slower) growth of 3B05 while reducing the pH of the medium. State ② commences when the pH hits a critical threshold (set by the pKa of acetic acid), which briefly stops the growth of 1A01 and 3B05. The low pH and high acetate concentration forces 1A01 into a state of acetate stress and the community into state ③. In this state, 1A01 excretes large amounts of glycolytic intermediates (e.g., pyruvate). This stress-induced excretion plays a key role in alleviating acetate stress, as it first allows 3B05 to grow slowly despite the low pH, and then rapidly as acetate is

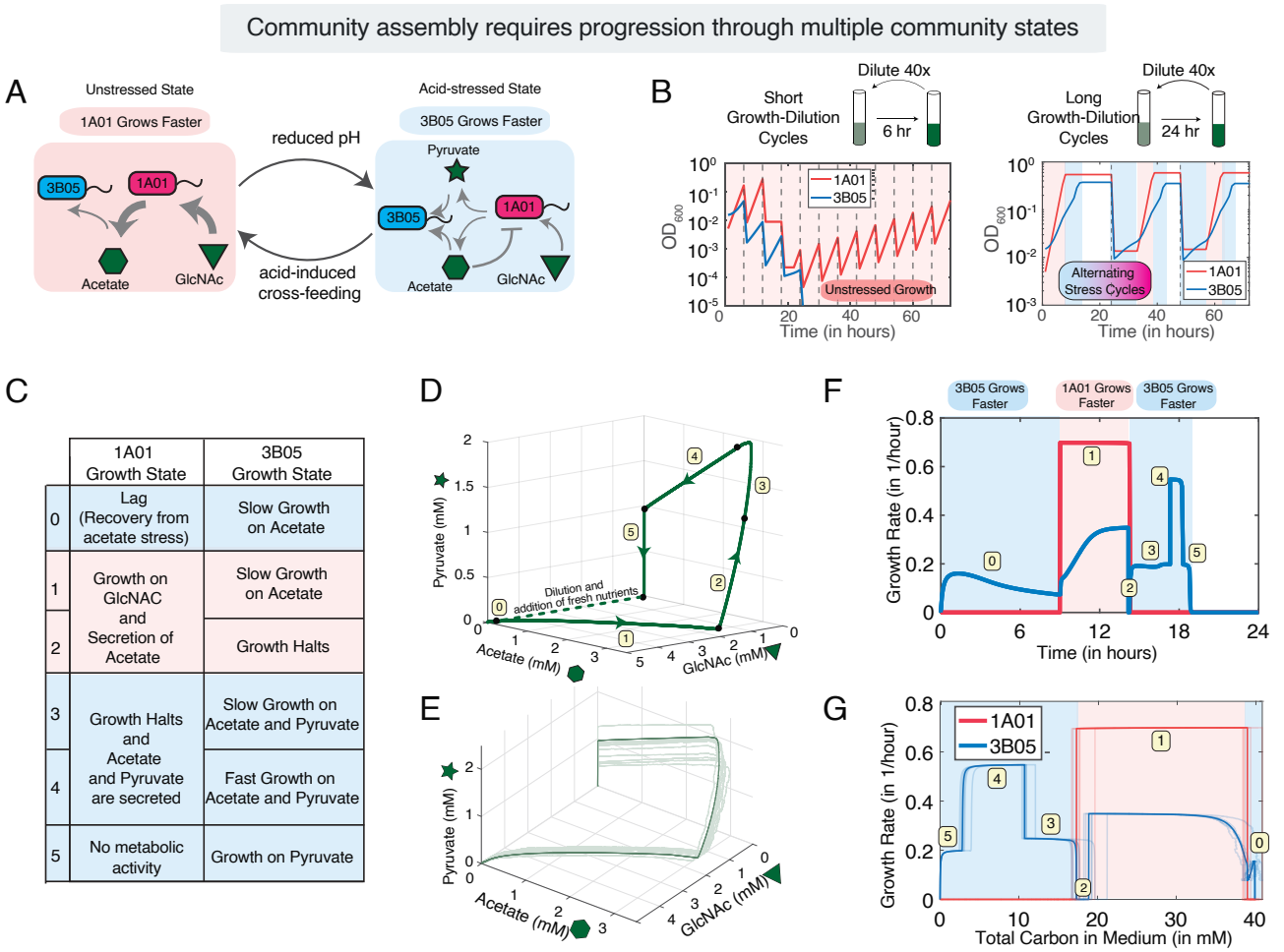

Fig. 1. Sequential transitions in a community's state revealed in a simple coculture of a sugar consumer and an organic acid consumer. (*A*) Schematics describing the dynamics of a coculture of marine bacteria *Vibrio* sp. 1A01, a sugar consumer, and *Neptunomonas* sp. 3B05, an organic acid consumer, growing on N-acetyl glucosamine (GlcNAc) under repeated serial-dilution cycles: the coculture passes from an initial unstressed state in which 1A01 grows faster than 3B05 (pink box), to an acid-stressed state in which 3B05 grows but 1A01 does not (blue box). Pointed gray arrows indicate metabolic flow (thickness indicates flow magnitude) and blunt-end arrows indicate growth inhibition. (*B*) Experimental investigation by Amarnath et al. (16) revealed coexistence only if serial-dilution cycles were sufficiently long to allow for an intricate sequence of community states, i.e., different combinations of the physiological states of each species and media conditions, labeled by the numbers in (*C* and *D*). Numerical data from a microscopic model simulating this experimental system is shown in (*B*) and (*C*) shows changes in three major metabolites in the numerical simulation while table (*D*) describes the community states along the green path in (*C*). (*E*) The growth rate of each species along the path in (*C*), i.e., between two serial dilutions (stable cycle shown). (*F*) Perturbed trajectories (light green in the space of metabolites in response to random perturbations of metabolites (±1% every 10 min). Unperturbed trajectory is in dark green. (*G*) Growth rate (light blue,red) along perturbed trajectories in (*F*) as a function of total carbon in the medium in that trajectory; for other potential eco-coordinates, see *SI Appendix*, Fig. S1.

consumed and pH creeps up (state ④). Although state ④ is very brief in time (<10% of the cycle, Fig. 1*E*), it accounts for about half of the increase of the biomass of 3B05 (*Right* panel, Fig. 1*B*) and is thus a key state in allowing the maintenance of 3B05 in the community. The high density of acetate-consuming 3B05 in turn leads to the near complete removal of acetate from the medium and the restoration of pH (state ⑤). The removal of acetate is crucial to save 1A01 from death, making it available for another round of growth when fresh nutrient arrives in the next cycle.

The above description of the dynamics makes it clear that the stability achieved through a cycle is not due to a "balancing" of different effects of the environment, as is presumed in canonical syntrophy. Rather, it results from a sequence of physiological states which conspire to arrange the growth of the two species in a staggered manner, with 1A01 growing first, and 3B05 growing later (after acetate stress prematurely stopped the growth of 1A01 while GlcNAc is still available). Thus, for this system the sequence of physiological states is an essential feature giving rise to the coexistence of the two species, and a coarse-grained steady-state description would necessarily miss the metabolic basis of coexistence.

Amarnath et al. (16) showed that this highly dynamical mode of coexistence is not specific to the marine species studied: dynamic coexistence through a similar physiological transition of acid shock and recovery was shown also for cocultures of species taken from a soil community or even between enteric and soil bacterium. Metabolic analysis in refs. 16 and 39 suggests that such interactions are generic between species with complementary sugar-preferring vs. acid-preferring bacteria, or between glycolytically oriented vs. gluconeogenically oriented modes of metabolism. Thus, dynamic coexistence with each species passing through multiple physiological states in a cycle may be the norm rather than the exception (12, 40–42). Importantly, such dynamic coexistence must be contrasted with coexistence due to specialized growth on different nutrients, where each species is relatively indifferent to presence or absence of the other species (43). In contrast, while 1A01 and 3B05 do grow on different nutrients, each species is strongly dependent

on the growth and nongrowth phases of the other, even if there are no common nutrients.

The lack of reports of such dynamical features of microbial communities may reflect the lack of time-resolved measurements. For the system studied in ref. 16, many important activities occurred within a 1 to 2 h window of the 24-h growth–dilution cycles (such states ④ and ⑤) and are difficult to catch. It may also be the case that the lack of dynamical measurements is itself a reflection of the bias on steady-state characteristics and stable coexistence of species, possibly biased by the large number of theoretic studies on steady-state properties starting with the pioneering work of MacArthur and May (23, 44).

A Top–Down Model for Complex Communities. To investigate cyclic community dynamics efficiently, we propose a general phenomenological model—the CS Model. In this model, we take the growth rate, $r_\alpha(\vec{S}(t))$, of each species α to depend on the community state $\vec{S}(t)$. The high-dimensional state $\vec{S}(t)$ includes all aspects described earlier, from the internal physiological states of microbes such as growth and nongrowth states to external spatial structure, and progresses through multiple states due to various environmental changes driven by the microbes themselves as illustrated in Fig. 2. The growth of a species α during the j^{th} cycle is described by

$$\frac{d}{dt}\rho_\alpha^{(j)} = r_\alpha\left(\vec{S}(t)\right)\cdot\rho_\alpha^{(j)}(t) \qquad for\ 0 \le t \le T. \qquad [1]$$

When t reaches the growth period T, all densities are reduced by a common factor $\delta < 1$, i.e.,

$$\rho_\alpha^{(j+1)}(t=0) = \delta\cdot\rho_\alpha^{(j)}(t=T). \qquad [2]$$

Eqs. **1** and **2** define an effective "map" for the density of each species at the beginning of each cycle, $\rho_\alpha^{(j)}(0)$ starting from the initial composition $\rho_\alpha^{(1)}(0)$. For convenience, we choose the growth period T to be sufficiently long such that the total cell density, $\rho_{\text{tot}}(T) \equiv \sum_\alpha \rho_\alpha(T)$, has time to reach the maximum ρ_{tot}^{max}, where $r_\alpha = 0$ for all species.

Eventually, the community might settle into a stable cyclic dynamics (referred to here as the "stable cycle") such that $\rho_\alpha^{(j)}(t=0) = \rho_\alpha^{(j+1)}(t=0)$ for all species α. We do not consider here alternative possibilities such as oscillations and chaotic states which are explored in refs. 45–48 but are uncommon in natural communities as well as theoretical models (49).

Goal of the top–down CS Model. Bottom–up models can attempt to compute the trajectory of the community state vector in the stable cycle, hereby denoted as $\vec{S}^{sc}(t)$, by modifying steady-state models such as the Lotka–Volterra model by including time-dependent interactions $A_{ij}(t)$ (50, 51) or the CR model with dynamic resource consumption or secretion rates (45, 52–55), etc. However, deriving $\vec{S}^{sc}(t)$ through such models requires a large number of parameters that is experimentally intractable to determine. The CS Model, a top–down model, does not seek to compute $\vec{S}^{sc}(t)$ but, instead, to derive self-consistency equations on $\vec{S}^{sc}(t)$, and exploit these consistency conditions to predict properties of communities that might be directly observed in experiments.

The low-dimensionality assumption. To counter the explosion of parameters experienced by bottom–up models that incorporate time dependency, we will assume that $\vec{S}^{sc}(t)$ admits a low dimensional description, i.e., community dynamics can be captured by a small number of variables. In particular, we assume that the system dynamics include a low-dimensional attractor to which trajectories rapidly converge under perturbations, and that these dynamics can be approximately described by coordinates on the attractor (48, 56, 57). In the extreme, if a single variable $\eta(t)$ (an "eco-coordinate") is sufficient, growth rate of species α, $r_\alpha(\eta(t))$, would depend on all other species and the environment only through the current value of $\eta(t)$. Below, we explore this extreme case and the resulting predictions.

Mechanistically, candidates for $\eta(t)$ include the amount of nutrients in the medium, the oxygen level (a major driver of metabolic activity), the pH of the medium (a measure of fermentation waste built up), the accumulation of quorum sensing signal, or other global characteristics that changes monotonically during community growth in a cycle. Note that the relation between the growth rates $r_\alpha(t)$ and $\eta(t)$ does not need to be mechanistically causal for our mathematical framework below, as long as environmental variables are sufficiently correlated over the stable cycle. A tight correlation between environmental variables might actually arise due to the stability of the stable cycle itself, or it might arise for mechanistic reasons such as mass conservation. Also, as we will discuss later, if individual species in a complex ecosystem each use simple regulatory strategies for their growth rate, the resulting community dynamics will necessarily be low dimensional with a good eco-coordinate, despite lacking a central (community-wide) coordinator.

As an example of the low-dimensionality of the trajectories that communities traverse, we perturbed the stable cycle in the simulation of the case study of 1A01 and 3B05 discussed above by shifting the metabolite levels randomly (± ∼1% every 10 min); the resulting trajectories are shown in Fig. 1*F*. We plotted the growth rate of the two species along these perturbed trajectories as a function of several putative eco-coordinates $\eta(t)$ such as concentrations of GlcNac, Pyruvate, GlcNac + Acetate; see *SI Appendix*, Fig. S1. While some of these choices show large variation in growth rate for the same value of η (e.g., η = pyruvate concentration), some choices result in highly reproducible curves despite fluctuations (e.g., η = total amount of carbon atoms consumed, as shown in Fig. 1*G*). These latter choices would make better eco-coordinates as they reflect monotonic and stable parameterizations of the trajectory. In particular, the plot in Fig. 1*G* shows visually almost two equal regimes, one dominated by the growth of 1A01 (early phase, with 20 to 40 mM C remaining) and another dominated by the growth of 3B05 (late phase, with 0 to 20 m C remaining).

Additionally, if all growth rates are nonnegative and $\partial\dot{\eta}(t)/\partial\rho_\alpha > 0$ holds for all species, then we have the nontrivial prediction (see *SI Appendix*, section S2E for details) that the system features a unique stable cycle which is attained asymptotically over repeated cycles (as long as all species are present initially). While this prediction precludes multistability (suggesting that no such one-dimensional eco-coordinate exists if alternative stable states, oscillations, or chaos are observed), it suggests that a feasible strategy for all species to guarantee their survival despite large demographic fluctuations is to coordinate their physiological response to environmental changes through a low-dimensional representation of the environment.

Self-consistency and stability. We now derive a self-consistency equation for the sequence of community states of the stable cycle, $\vec{S}^{sc}(t)$, in the form of a stability condition. In a stable community, after one cycle, the gain in cell density due to growth over a cycle balances the dilution at the end of the cycle for each surviving species α. This provides the following condition for stability:

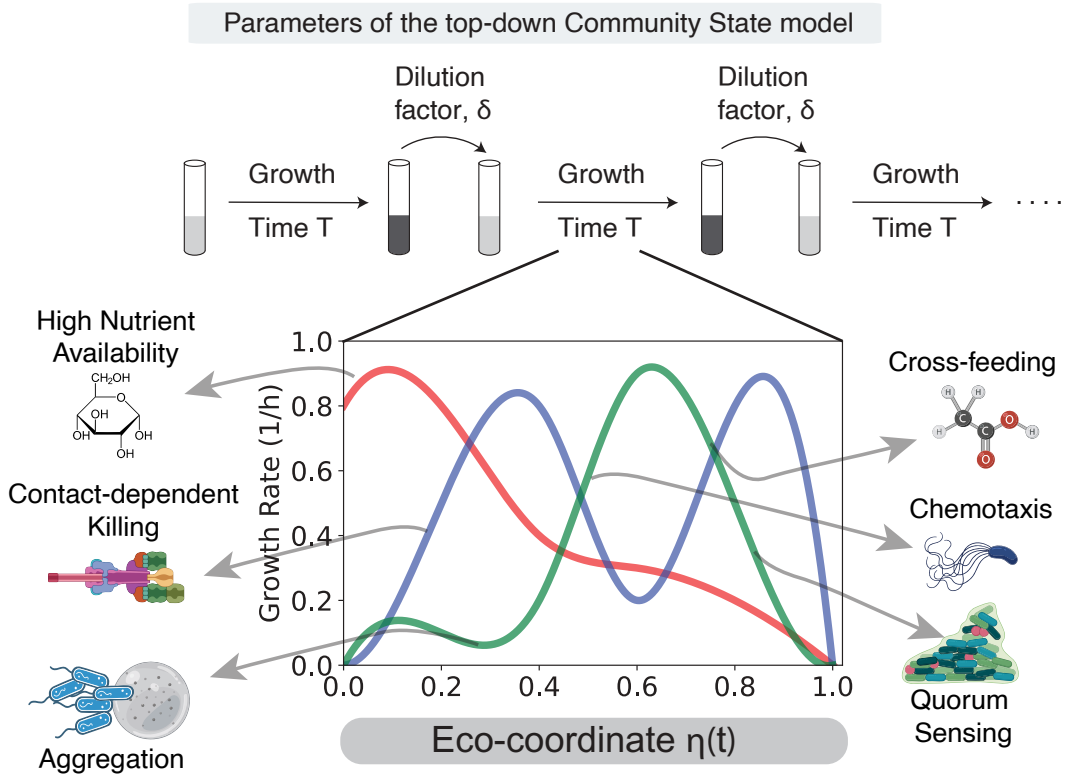

Fig. 2. Top–down description of ecosystems with time-dependent interactions in the CS Model. Metabolic and other activity in microbial ecosystems can lead to accumulating toxins, creation of spatial structure and creation or depletion of nutrients over time. These internally driven changed environments lead to physiological changes in the microbes which can change how they interact with each other or with nutrients. As a consequence, species go through periods of growth and no growth at different times. We model ecosystems that grow, gaining biomass for a period T, before being diluted into a fresh environment. During the growth period, the community changes its environment through many complex processes shown, leading to a sequence of community states. The CS Model assumes these processes to be turned on and off at different points along a one-dimensional phenomenological coordinate $\eta(t)$ that parameterizes the sequence of community states. In specific systems, $\eta(t)$ might parameterize nutrient depletion, buildup of toxins, and spatial structure, etc. As suggested by the cartoon, different species might dominate at different $\eta(t)$.

$$\int_0^T r_\alpha(\vec{S}^{sc}(t))dt = -\log(\delta), \text{ for all } \alpha. \quad [3]$$

Under the low dimensionality assumption, through a simple change of variables from t to η^{sc}, this stability condition can be written as (see *SI Appendix*, section S2E for details),

$$I_\alpha \equiv \int_{\eta^{sc}(0)}^{\eta^{sc}(T)} \frac{r_\alpha(\eta^{sc}(t))}{d\eta^{sc}/dt} d\eta^{sc} = -\log(\delta). \quad [4]$$

Biomass as an eco-coordinate. Eq. **4** is not immediately useful as it is not a closed equation—$d\eta^{sc}(t)/dt$ appears explicitly but $\eta^{sc}(t)$ is not known without a bottom–up mechanistic model and many specific assumptions on time/state-dependent interactions. In our top–down approach, we make an alternative assumption that allows for a closed, self-consistent description: we take the eco-coordinate to be the community biomass during the cycle, i.e.,

$$\eta^{sc}(t) = \rho_{\text{tot}}(t), \quad [5]$$

where $\rho_{\text{tot}}(t)$ is determined from r_α via

$$\rho_{\text{tot}}(0) = \sum_\alpha \rho_\alpha(0) \text{ and } \frac{d\rho_{\text{tot}}(t)}{dt} = \sum_\alpha r_\alpha(\rho_{\text{tot}})\rho_\alpha. \quad [6]$$

Thus, unlike other choices of the eco-coordinate $\eta(t)$, which require knowing the sequence $\vec{S}^{sc}(t)$, the assumption (Eq. **5**), which makes the growth rates r_α depend on the biomass, can be viewed as the minimal closure of the ecosystem dynamics.

The assumption (Eq. **5**) converts the local stability criterion of Eq. **4** to a global criterion (*SI Appendix*, section S2E) for any nonnegative $r_\alpha(\rho_{\text{tot}})$. For the specific case of a two-species community, A and B, the criteria for coexistence is given by

$$I_{A,B} \equiv \int_{\delta\cdot\rho_{\text{tot}}^{\max}}^{\rho_{\text{tot}}^{\max}} \frac{r_A(\rho_{\text{tot}})}{r_B(\rho_{\text{tot}})} \cdot \frac{d\rho_{\text{tot}}}{\rho_{\text{tot}}} > \log(1/\delta). \quad [7]$$

and similarly $I_{B,A} > \log(1/\delta)$. This two-species criteria were previously studied by refs. 52 and 58 in the context of resource competition with Michaelis–Menten saturation kinetics. We discuss generalizations to multispecies ecosystems later.

Before exploring the consequences of the stability criterion Eq. **7**, we address some features and limitations of our assumption of biomass being the eco-coordinate. First of all, we note that assumption can be justified mechanistically in a number of cases, e.g., diauxic shift, quorum sensing, acid shock (*SI Appendix*, section S2B and Figs. S2 and S3). For more complex systems such as the example of 1A01–3B05 interaction discussed above, we see that total carbon remaining, which is essentially the negative of the total mass of 1A01 and 3B05, i.e., ρ_{tot} of this system, serves empirically as a good eco-coordinate (Fig. 1*G*). We expect this to be broadly true as the growth yields in bacteria are not that different for different carbon sources (59).

Other advantages of using biomass as an eco-coordinate are illustrated in Fig. 3: for example, biomass naturally emphasizes

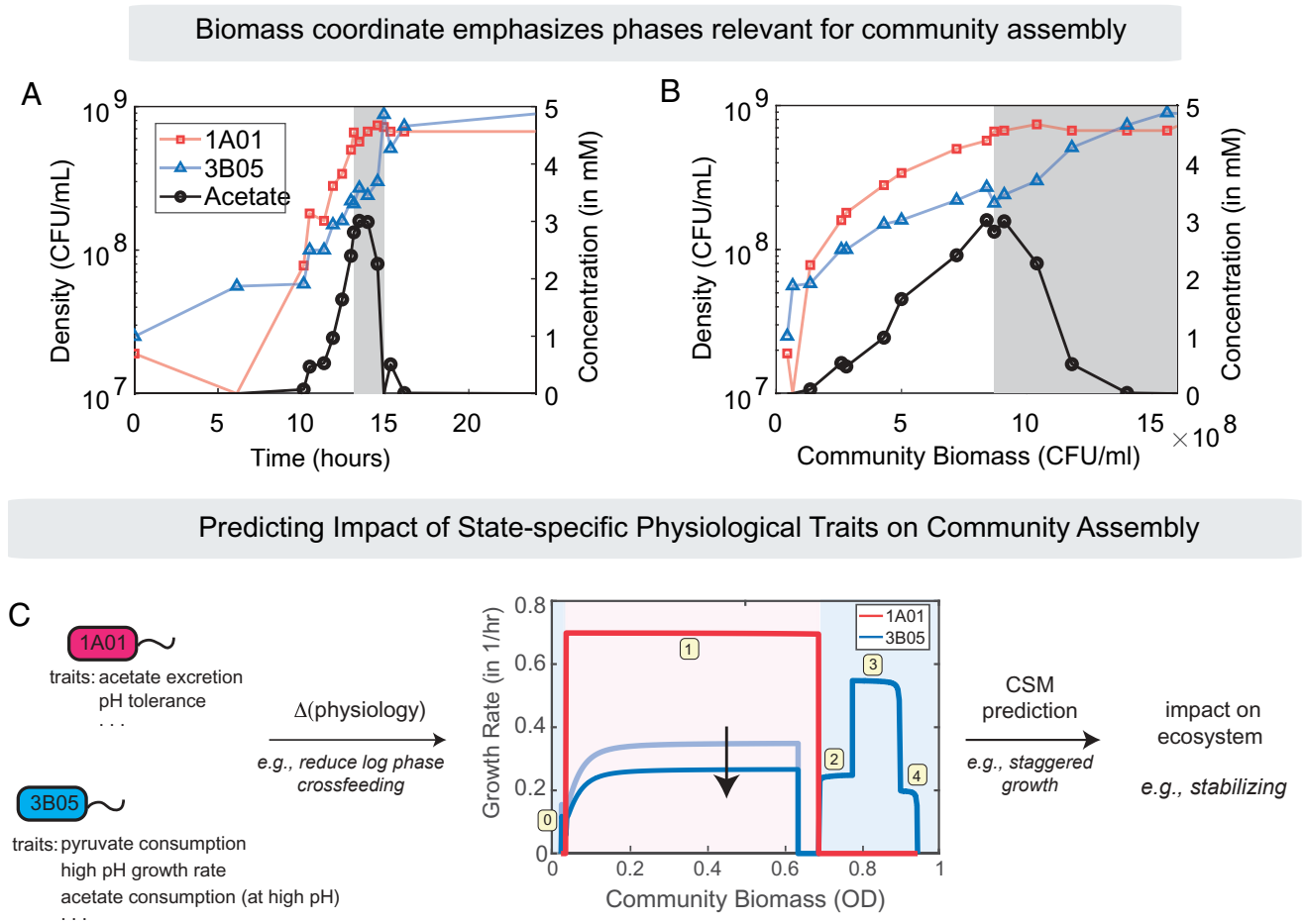

Fig. 3. Benefits of indexing community states by the accumulated community biomass. (*A* and *B*) Experimental data from ref. 16 on cell densities and acetate concentration during a growth dilution cycle. (*A*) Key physiological shifts driving coexistence in ref. 16 occur in a brief (gray) time window marked by acid stress-induced changes in acetate (black curve). Uniform real-time sampling may miss this window and overrepresents other phases. (*B*) In contrast, sampling by community biomass emphasizes the gray region, highlighting dramatic metabolite changes that help reveal the mechanisms of community assembly. (*C*) The ecological impact of a mutation that changes physiological traits in specific environments (here, reducing log phase crossfeeding) can be hard to predict in bottom–up models. In the CS Model, that trait's impact is seen as a shift in growth rate in a specific community state (here, 3B05's light blue growth curve becomes dark blue in the pink community state). The model's key equations (Eq. **7**) link these growth rate shifts to coexistence, and predict the mutation's effect on community assembly (here, reduced log phase crossfeeding results are predicted to increase stability due to more staggered growth).

growth phases most relevant for community assembly. As shown in Fig. 3*A*, when plotted in real time, the most critical physiological changes occur in a brief period indicated by the gray band (where acetate build-up hits a threshold, leading to subsequent stress-induced crossfeeding of pyruvates and other metabolites). Based on the growth curves alone (red and blue symbols) and without acetate data (black symbols), there would not have been any reason to sample the short time period within the gray band in Fig. 3*A* where multiple layers of cross-feeding took place (16). In comparison, the time domain emphasizes state ⓪ and the state after ⑤ in Fig. 3 where little biological activities took place, while the all-important state ④ is largely neglected. In contrast, when plotted against the total biomass (Fig. 3*B*), we see a clear regime where 3B05 grows, catching up to and exceeding 1A01.

Biomass-based results like Eq. 7 also offer an intuitive framework to predict the effects of physiology-altering mutations that would be difficult to predict from a microscopic bottom–up model. For example, consider a physiological change in 3B05 that reduces its early-phase growth rate as shown by the downward arrow in Fig. 3*C*. Although a naive expectation might be that reduced growth on the cross-fed metabolite acetate would destabilize coexistence—since cross-feeding is thought to promote coexistence (12)—the biomass-based result in Eq. 7 predicts the opposite. Specifically, as analyzed further below, reducing cogrowth in biomass intervals favors coexistence by ensuring each species achieves sustained (but capped) growth in the community state it dominates.

We note that the precise sequence of community state $\vec{S}^{sc}(t)$ can depend on external parameters like initial supply of nutrients, dilution factor δ. This dependence is not a limitation of our framework since we do not seek to predict the sequence of state $\vec{S}^{sc}(t)$ (as sought by bottom–up models); instead, we merely seek self-consistency equations (Eq. 7) that this stable cycle of states must satisfy. On the other hand, indexing by biomass does have limitations in its inability to capture biological effects such as cell death or lag phases after saturation, or environmental changes not associated with or driven by growth (45, 46, 60).

CS Model with Staggered Growth Dominance. Let us consider a toy model of a two-species community with staggered growth dominance. In this model, the growth functions $r_A(\rho_{tot})$, $r_B(\rho_{tot})$ are step-like as shown in Fig. 4*A*: species *A* grows faster than *B* for biomass ρ_{tot} below a threshold value ρ^c_{tot}, with growth dominance

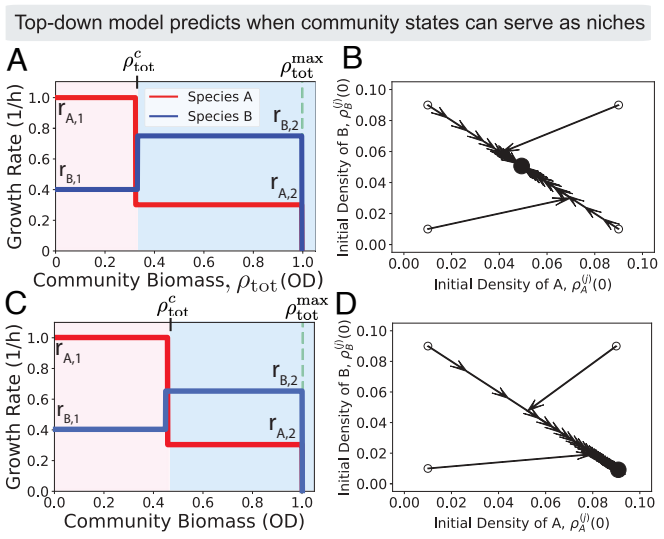

Fig. 4. Toy Model with staggered growth dominance predicts coexistence of species. (*A*) Growth curves $r_X(\rho_{tot})$ for two species; species *A* grows rapidly in the early community state that lasts for community biomass $\rho_{tot} < \rho_c$; species *B* grows faster when $\rho_{tot} > \rho_c$. (*B*) Species densities at the end of consecutive serial dilutions from different initial conditions (black open circles) for growth curves in (*A*) converge to a stable coexistence point (black solid circle). (*C* and *D*) Same as (*A* and *B*) but the modified growth curves in (*C*) lead to extinction of species *A* shown in (*D*). While growth curves in (*A*), (*C*) are visually similar, Eqs. **8** and **9** predict that the two community states can support two species in (*A*) but not in (*C*).

in this region quantified by $p_1 \equiv r_{A,1}/r_{B,1}$. Conversely, species *B* grows faster for $\rho_{tot} > \rho^c_{tot}$, with growth dominance $p_2 \equiv r_{B,2}/r_{A,2}$. This model can be viewed as a simplified version of the 1A01–3B05 system discussed above (compare Fig. 4*A* with Fig. 3*E*, with total carbon being the opposite of ρ_{tot}).

It is tempting to interpret the two biomass intervals defined in this model, $\rho_{tot} < \rho^c_{tot}$ and $\rho_{tot} > \rho^c_{tot}$ as two dynamic "niches." As each such niche is dominated by one distinct species, one might expect the two species to coexist over many serial dilutions. This is of course the case if the growth dominance of each species in its niche is infinite, i.e., for $r_{B,1} = 0$ and $r_{A,2} = 0$, but not necessarily if the growth dominances are weak, e.g,. $p_1 \approx 1$ and $p_2 \approx 1$. Applying the mutual invasibility condition Eq. **7** to the model of Fig. 4*A* gives us the precise conditions for stable coexistence:

$$p_1 \cdot \log(\rho^c_{tot}/(\delta \cdot \rho^{max}_{tot})) > \log 1/\delta - p_2^{-1} \cdot \log(\rho^{max}_{tot}/\rho^c_{tot}), \quad [8]$$

$$p_2 \cdot \log(\rho^{max}_{tot}/\rho^c_{tot}) > \log 1/\delta - p_1^{-1} \cdot \log(\rho^c_{tot}/(\delta \cdot \rho^{max}_{tot})). \quad [9]$$

When the growth dominances p_1, p_2 and the width of biomass interval ρ^c_{tot} satisfy these conditions (Eqs. **8** and **9**), serial dilution cycles starting from any initial condition converge to a unique fixed point where both species are present; see e.g., Fig. 4*B*. Generally, the state of the community in the stable cycle is characterized by a coexistence ratio, defined as $\phi \equiv \frac{4\rho_A \cdot \rho_B}{(\rho_A+\rho_B)^2}$, which is 1 in the example shown. Outside of this regime, e.g., with visually similar growth functions shown in Fig. 4*C*, one of the two species goes extinct over multiple cycles (i.e., ϕ=0) as shown in Fig. 4*D*. See *SI Appendix*, section S2D and Fig. S4 for more analyses.

Thus the nature of niches that arise from community states with staggered dominance is not immediately transparent—what is the impact of the width of biomass intervals over which a community state persists, what effect does their temporal ordering have, and can such staggered dominance support complex communities with many species? The phenomenological CS Model can be used to address these questions and makes nontrivial predictions on how growth and nongrowth states should be structured across a community for the stable coexistence of its members. Below, we highlight three insights derived from Eqs. **8** and **9** into the nature of these dynamical niches for communities of two and more species with staggered dominance.

Tolerance to growth dominance. In steady-state models, dominant growth of a species on a nutrient precludes other species growing on that same nutrient (44, 61). However, this is not so in the CS Model with staggered growth dominance. Consider the two-species, two-interval toy model again. As shown in Fig. 5 *A* and *F*, as the growth dominance p_1 of species *A* in the first biomass interval increases from 1, the coexistence ratio ϕ does increase but saturates at $\phi < 1$, indicating that the other species is not extinguished even as $p_1 \to \infty$. The saturation value of ϕ is dependent on p_2, the value of growth dominance in the other regime (Fig. 5, see exact analytical results in *SI Appendix*, section S2D). This reveals the origin of the tolerance of coexistence to growth dominance in the CS Model: dominance in one community state does not necessarily extinguish others because they can thrive in other community states.

The tolerance to growth dominance seen in this model contrasts with a basic tenet of ecology, that species utilizing resources efficiently will drive other species to extinction. This notion, which is at the root of the "paradox of the plankton" (62), arises largely from analysis of steady-state models for which all species grow at a single rate in the steady state. It is such a steady-state perspective that raises questions about the coexistence of

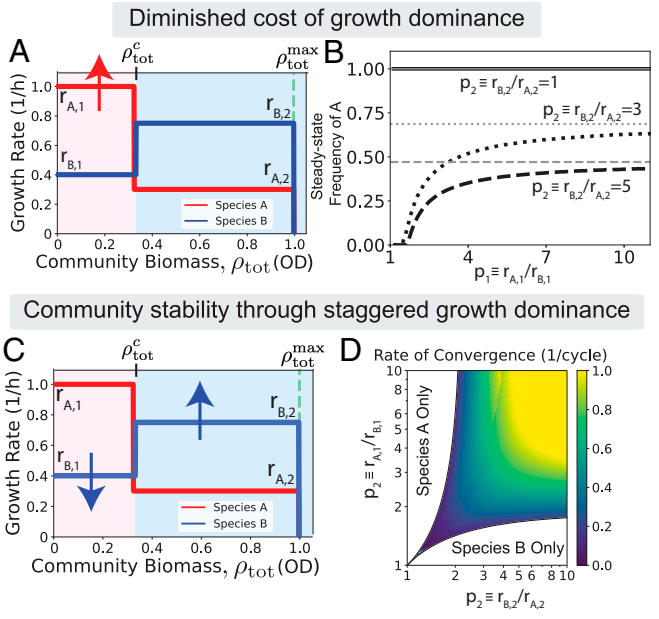

Fig. 5. Key features of community states as niches. Starting from the parameters in the toy model presented in Fig. 4, (*A*) we increase growth dominance $p_1 = r_{A,1}/r_{B,1}$ of species *A* in the first community state. (*B*) Stable-cycle abundance of species *A* as a function of growth dominance p_1 shows a quickly saturating effect. The black (solid, dotted, dashed) lines are values (computed numerically and analytically) for $p_2 = 1, 3, 5$ respectively, and the gray lines are the asymptotic values as $p_1 \to \infty$. (*C*) We consider a coordinated change of growth dominance p_1, p_2 across multiple community states. (*D*) Rate of convergence back to stable coexistence point (i.e., Lyapunov exponent of stability) as a function of growth dominances p_1, p_2; ecosystem stability increases without saturation for coordinated changes in dominance.

slow-growing species in a community, e.g., 3B05 in the example of Fig. 1. In contrast, staggered growth allows individual species with significant growth advantages in one community state to coexist with other slower species (thus retaining "services" by the latter in other more challenging community states). This effect will play a pivotal role in the coexistence of larger communities to be described below.

Stability through coordinated dominance. While coexistence tolerates strong individual growth dominances as described above, the coexistence regime is broadened if *both* p_1 and p_2 are large, see *SI Appendix*, Fig. S5. This effect is seen also in the robustness of coexistence, measured by the convergence rate to the stable cycle following small perturbations (the Lyapunov exponent); see Fig. 5 *C* and *D*. This metric is also a measure of the stability of the ecosystem against environmental or physiological fluctuations.

Since enhancement in the size and stability of the coexistence region requires increases in growth dominance in distinct community states (i.e., p_1 and p_2), such a communal effect is aided by different species coordinating their growth dominance across multiple community state. However, individual species can also contribute to this coordination, as a species can increase the growth dominance of another species in its dominant growth interval by reducing its own growth in that interval; e.g., species *A* can increase p_2, the dominance of species *B* in state 2, by decreasing $r_{A,2}$. Thus, this global coordination can be facilitated by individual species specialized to dominate in distinct community states.

Increased dominance requirement for late-growing species. The coexistence criteria $I_{A,B}$, $I_{B,A}$ are not symmetric between species *A* and *B*. This asymmetry can be traced to a "priority effect" where species *A* capitalizes on early growth, accumulating large numbers while species *B*'s growth occurs in a later biomass interval (55, 63, 64). The consequences of this priority effect are shown for an *N*-species community in Fig. 6 *A* and *B*: if each species is dominant in a unique biomass interval of equal width (with equal value of growth dominance p in each community state), late-growing species are driven extinct after several cycles.

We find that members of such a community can all coexist despite the priority effect if early-growing species occupy narrower biomass intervals. Based on Eqs. **8** and **9**, we were able to derive a special distribution of biomass interval (*SI Appendix*, section S2H) for coexistence. Expressed in the normalized biomass coordinate $\eta = \rho_{\text{tot}}/\rho_{\text{tot}}^{\max}$, we find that for each species in the community to exist at equal frequency, then the width interval $\Delta\eta_n$ for the species growing in the nth-interval must be exponentially large, with

$$\Delta\eta_n \sim (1/\delta)^{n/(N+p-1)}, \qquad [10]$$

provided that growth dominance p does not greatly exceed N; see Fig. 6 *C* and *D*. Thus, appropriate choices of growth intervals can counteract the priority effect. Alternatively, the priority effect can be counteracted by stronger growth dominance of the late-growing species even if the biomass intervals of the different states are equal; see *SI Appendix*, Fig. S8 and ref. 55. These results underscore and quantify the large (exponentially increasing) burden faced by late-growing species to be included stably in large communities.

CS Model with Overlapping Growth Dominance. In a many-species community, it is unlikely that the intervals for dominant growth for different species would be perfectly staggered as depicted in Fig. 6*C*. In this section, we relax the staggering constraint, allowing the growth preference of different species to overlap in multiple community states (i.e., in multiple biomass intervals). This allows different species to compete in the same community state. We model this effect by a "preference matrix" where each element of the matrix denotes the community state in which each species can grow fast or slow (the "growth preference"), with the boundaries of the community states taken to be the same for all species (given by defined biomass values (η_{i-1} and η_i for the ith community state). We allow for each species to grow preferentially in any community state, so that we can assess the effect of competition between species growing preferentially in the same community states.

We first explored the case where each community state can support the rapid growth of a fixed number K_s of species. An example of a preference matrix is shown in Fig. 7*A*; each community state was assumed to take the same average interval $\Delta\eta$ of biomass. In each community state (i.e., column of matrix shown), we assigned a high growth rate r_+ for K_s randomly chosen species and a low growth rate r_- that is a $p = 100$ times lower than r_+ for all other species. 30% random variation added to each parameter; see *SI Appendix*, section S2I. The results, shown in Fig. 7*B*), display an expected decrease in stable-cycle diversity with an increasing number of species K_s competing in each community state. However, the decrease in surviving species is slower than a naive expectation of N/K_s.

To gain insight into which species survive, contrast rows of the matrix corresponding to surviving (blue) and extinct species (red) in Fig. 7*A*. Survivors (blue) tend to grow fast in five or more community states while extinct species (red) have mostly three preferred states. To test this hypothesis, we plotted the average number of preferred states (states in which a species grows at r_+) for the surviving and extinct species for the $N = 100$ system

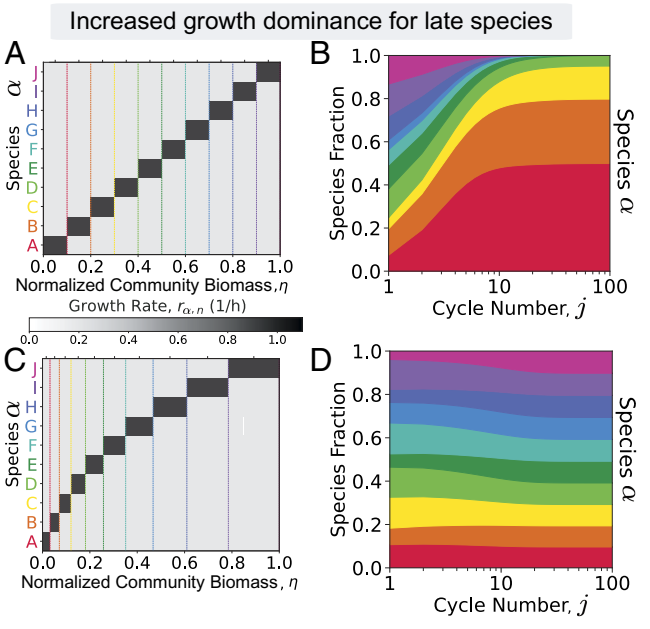

Fig. 6. Staggered CS Model reveals late species must feature increased growth dominance to survive. (*A*) A 10-species ecosystem with each species "dominant" with high growth rate r_+ in a unique community state and r_- elsewhere; all community states last equal intervals of normalized community biomass $\eta \equiv (\rho_{\text{tot}}/\rho_{\text{tot}}^{\max} - \delta)/(1-\delta)$. (Here δ is the dilution factor between growth cycles. Growth dominance $p = r_+/r_- = 5$.) (*B*) Stacked chart shows species abundance at the end of each cycle (in fraction of total biomass) over multiple serial-dilution cycles. (*C* and *D*) Same as (*A* and *B*) but with wider biomass intervals for later community states (Eq. **10**). The wider intervals for later species compensate for the priority effect enjoyed by early species.

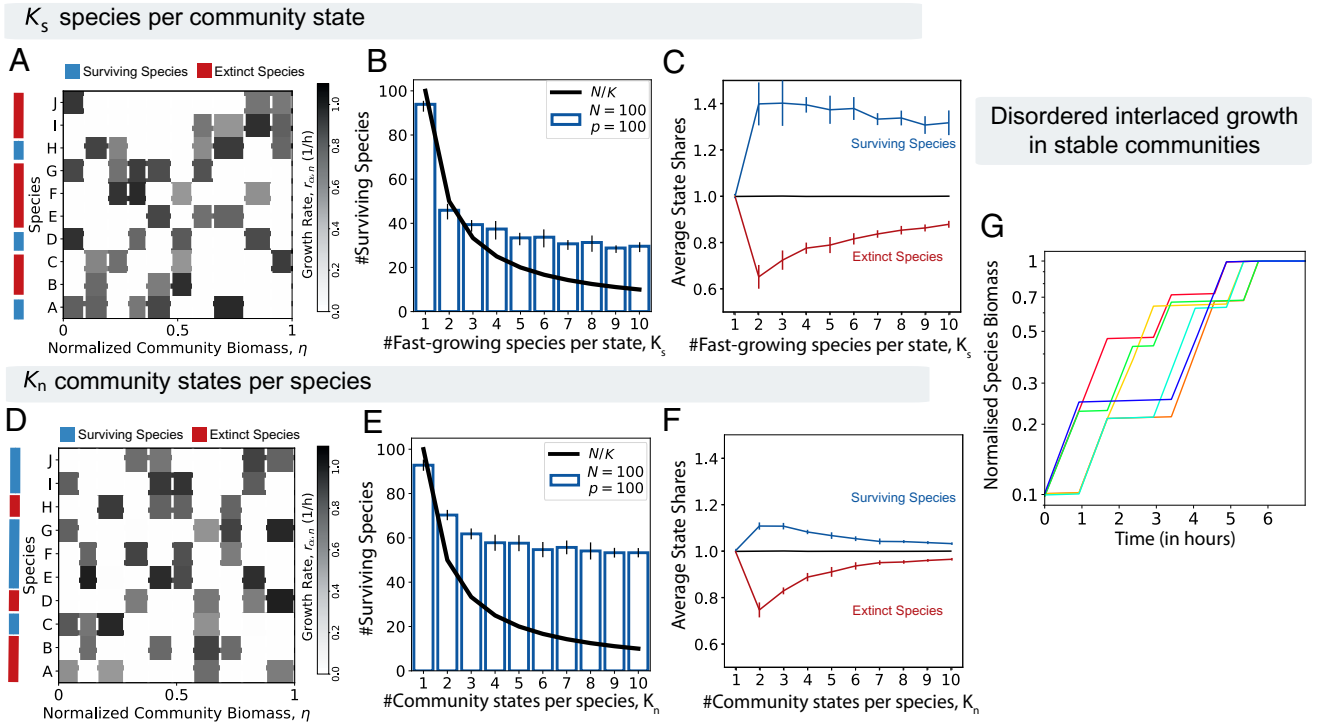

Fig. 7. Competition and coexistence in complex communities. (*A*) K_S model of random preferences: K_S randomly chosen species are given high growth rate r_+ in each community state that lasts for a fixed interval of community biomass η; all other species are set to slow growth r_- in that interval. Illustrative example shown in (*A*) with $K_S = 4$, $N = 10$ total species and growth dominance $p = r_+/r_- = 100$. After many serial-dilution cycles, some species persist (blue) while others go extinct (red). (*B*) Average number of surviving species with $N = 100$ exceeds naive expectation N/K_S (black line). (*C*) The average number of "state shares" for surviving species and extinct species as a function of K_S; here, state share is the share of community states that each species grows quickly in. For example, Species A in Fig. 5*A* receives 1/4 of each state in grows quickly as it shares the fast growth with three other species, and thus has a total of 1.25 state shares. (*D*) K_n model of random preferences: each species is assigned a high growth rate r_+ in K_n randomly chosen community states and slow growth r_- in other states. Illustrative example shown with $K_n = 4$, $N = 10$. (*E* and *F*) Same as (*B* and *C*) but for the K_n model. (*F*) Average number of state shares for surviving species and extinct species as a function of K_S; state share is defined as in (*C*), but here each species may share each state with a different number of species. (*G*) Time course of normalized biomass for the surviving species over a stable cycle in an illustrative example of 10 species with $K_S = 4$ preferred niches and $K_n = 4$ competitors in each niche (imposing constraints of both K_S and K_n models). Species show a complex disordered pattern of growth and no-growth states with subtle correlations that enable coexistence. (Error bars in all panels indicate SD from 10 simulations of different growth matrices with 30% variation in r_+, r_-, and $\Delta\eta$) .

(Fig. 7*C*); we see that the surviving species are generalists who can grow rapidly in multiple community states.

We next explore the situation where each species has a fixed number K_n of preferred states, i.e., now, all species are generalists to an equal extent. However, the identity of the preferred community states for each species is randomly chosen; see Fig. 7*D* for an example matrix. The number of surviving species is now clearly increased compared to the K_s model; compare Fig. 7*E* to Fig. 7*B*. What factors distinguish the surviving and extinct species? The specific example in Fig. 7*D* suggests that extinct species had more competitors in their preferred community states. To confirm this, we calculated the average number of preferred states for each species, weighted by the number of competitors that also grow fast in that state. Plotting this competition-weighted average state share for the $N = 100$ system, we find the surviving species (blue) indeed have a higher share of their preferred community states compared to extinct species (red) (Fig. 7*F*). Trajectories of species abundances (Fig. 7*G*) show that the dynamics in such systems no longer follow orderly succession dynamics but instead, show a seemingly disordered array of growth curves that are nevertheless cyclic and hence maintain coexistence.

In *SI Appendix*, Figs. S9 and S10 and section S2J, we consider a Consumer Resource model in a chemostat with each species growing on multiple resources. We explored similar constraints as above, with the total number of species growing on each resource (K_s) fixed or the number of resources each species grew on (K_n) fixed. We find that the fraction of surviving species for fixed K_n (43% for $K_n = 10$) is lower than in the CS Model (52% for $K_n = 10$) and higher for fixed K_s (34% for $K_s = 10$) than in the CS Model (28% for $K_s = 10$).

Discussion

In this work, we investigated models of microbial growth and survival in communities undergoing repeated cycles of environmental fluctuations with prolonged periods between nutrient replenishments, as seen in the wild (36, 65) and in serial-dilution lab experiments (12, 39, 66). Under these conditions, exponential steady-state growth is unsustainable due to resource consumption, waste accumulation, and other processes that speed up exponentially in time.

Predicting dynamics in such cyclic systems from bottom–up models is challenging, given our limited understanding of microbial behaviors beyond exponential growth (65, 67). Here, we developed a top–down CS Model, by assuming that the cyclic dynamics are low dimensional; we exploited the simplest closure of equations, namely that total biomass is the low dimensional eco-coordinate. We discussed the justifications for these assumptions, using a recent experimental investigation (16) as a case study. We derived quantitative self-consistency conditions on dynamical behaviors of community members

after repeated serial-dilution cycles, requiring the input of only several experimentally measurable quantities: the instantaneous growth rates of community members $\{r_\alpha(t)\}$ and the total biomass $\rho_{\text{tot}}(t)$.

In theoretical ecology, it is common to "coarse-grain" or ignore dynamics seen in real systems for the sake of "simplicity" (68, 69). However, the work here shows such coarse-graining a) destroys the link between physiology and ecology and b) overlooks an important source of niches. For (a), we note that the classic work on seasonal resources by Stewart and Levin (58) was dismissed as a mathematical observation without broad physiological relevance, but our work argues that their mechanism of dynamic coexistence is the essential link between physiology and ecology. We find that dynamic niches are more relevant given the complex physiology and nonlinear growth dependencies in real microbial ecosystems (12, 16, 17). For (b), we have quantified how physiological states can serve as dynamic niches. One major finding here is that community states differ from resource niches where many species can coexist by specializing on different resources, almost indifferent to the presence of other species: the dynamic nature of community states implies that the growth of one species strongly affects the growth of another. Our self-consistency criteria (Eq. 7) quantify dynamic niche overlap, with their explicit dependence on growth rate ratios serving as a fitness-like measure in dynamic contexts.

Our main results on physiological states as niches are as follows: 1) *Community stability through coordinated staggering of growth dominance:* Coordinating to stagger the fast growth phases of different species across distinct community states—rather than growing simultaneously—ensures stable coexistence. 2) *Tolerance to growth dominance:* increasing the growth rate of an individual species in its favored state does not necessarily eliminate other species and does not impact community diversity. 3) *Increased requirement on growth dominance for late-growers:* species growing in late community states must grow (exponentially) faster or grow for (exponentially) larger biomass intervals than species in early states.

A key strength of our model is its anchoring on experimentally accessible quantities rather than inaccessible interaction parameters. Instantaneous growth rates of individual species can be obtained from transient changes in species abundances (via e.g., 16S sequence as proxy), and the total community biomass can be obtained by measuring total protein or total RNA as proxies, or simply by the optical density if the culture does not aggregate. This allows the investigation of community dynamics to go beyond taxonomic characterization, and without invoking numerous fitted "interaction" parameters such as those employed in Lotka–Volterra or CR models, but based directly on the quantitative analysis of the dynamic data. For example, suppose a community is observed to exhibit a certain dynamical sequence $\{r_\alpha(t)\}$ for one cycle, can this sequence persist after repeated serial dilution cycles? For a community that settles down to a stable cycle with $\{r_\alpha^{sc}(t)\}$, do the data capture all the major species? And, might data from some important time intervals be missing? Concrete predictions of the CS Model, e.g. late species require increased dominance to survive, can be tested experimentally by acquiring dynamic growth data. In this sense, the CS Model is a phenomenological model that can be updated directly from data.

Our approach shares common elements with other top–down approaches like the Stochastic Logistic Model (70, 71) and recent data-driven models (72, 73) without explicit interspecies interactions. However, unlike these other models which attribute growth rate fluctuations to external factors, our model focuses on endogenously driven changes. Our model can be extended to incorporate external fluctuations perturbing growth niches across hosts or cycles, predicting abundance distributions as in ref. 70. A key distinction is that our approach imposes closure conditions on cycle-to-cycle growth rate variations to ensure stable but dynamic coexistence.

We also distinguish our findings from the well-known Storage Effect (43). While both the CS Model and the Storage Effect provide mechanisms for stable coexistence through negative frequency-dependent selection arising due to differential responses to the environment, the Storage Effect concerns exogenous temporal fluctuations near an equilibrium community while the CS Model concerns deterministic and endogenous temporal variations. The CS Model is in fact more similar to "classical coexistence mechanisms" such as resource partitioning or differential predator pressures (74), as it implicitly admits different environmental limiting factors such as nutrient supply, pH change, signaling molecules, etc. in the form of different community states. As such, the Storage Effect and the CS Model are not mutually exclusive either.

A key notion in our work is the existence of global community states with a low dimensional parameterization, the eco-coordinate $\eta(t)$, that can be sensed by microbes in that community. Our results suggest that it would be advantageous for organisms to use this information to adjust their behavior and grow in specific community states since such regulation would increase their chance of survival in the community. For example, organisms occupying early phases of the cycle may benefit from limiting their own growth there, so as not to eliminate other species active later in the cycle, those which could help the survival of all species in later phases of the cycle—as is the case for acid-induced stress relief (16), the early blooming acid-producing sugar eater is rescued from death by the late-blooming acid consumer which removes the excreted acid and detoxifies the environment. In this light, the acid consumer can be viewed as "public good" for the community, and the puzzle of species coexistence can be viewed as a problem of coordination around a public good. A possible future direction employing the CS Model would be to explore how diverse communities are robust to cheater strains that seek to maximize growth while impacting community diversity. Our findings already present possible explanations such as the tolerance of community diversity to growth dominance and greater stability through coordinated dominance, which suggest that species seeking optimal growth within their dynamic niche do not affect community diversity, and species seeking long-term survival instead benefit from specializing in their niche. However, these explanations currently lack physiological justifications constraining the ability of species to grow quickly in multiple dynamic niches.

We believe this eco-coordinate-based regulation hypothesis is biologically plausible: first, a number of key physiological parameters, e.g., pH, oxygen content, waste products, and iron availability, change with the accumulation of community biomass (75), and the values of these parameters to cause transitions in the physiological states of individual organisms are known. Second, it is known that several autoinducers are produced and sensed by a wide range of both gram-positive and gram-negative bacteria (76–78). In fact, AI-2 has been proposed to serve as a "universal signal" for interspecies communication (79–81). Third, it is common for microbes to develop sensors to detect important features of their environment (82–85); as total community biomass is clearly an important dynamical variable that can be used to forecast the fate of the community (e.g., how close to the

carrying capacity), it would not be surprising if organisms have evolved schemes to sense the total biomass. Various bacterial species may detect additional features of the community state, possibly in species-specific manner, and integrate the available information through regulatory mechanisms. In fact, in the case of bacterial toxicity, it has been shown that regulation of toxin production is associated with local biomass using experimental data (86), an optimal strategy according to evolutionary simulations (87–90), and a strategy found to afford fitness benefits experimentally (91).

Thus we can speculate, inspired by the CS Model, that organisms might actively regulate their own physiology by sensing low-dimensional, community-wide signals and thus organize stable ecosystems despite lacking an obvious central organizer for the community. Indeed, the existence of a group of organisms that can sense and respond to common low-dimensional features in the environment may be taken as a key characteristic that defines a "community."

Materials and Methods

All numerical results in Figs. 1 and 3 were obtained by simulations performed in Matlab (code available at https://github.com/avaneeshnarla/dynamic-metabolic). All other results were obtained using simulations performed in Python 3 using forward Euler integration. For the results in Figs. 4 and 5, the integration was performed in time with a growth period of 20 units and a time resolution of 0.001 units. For Figs. 6 and 7, the integration was performed in the normalized biomass coordinate (η) ranging from 0 to 1, with a resolution of 0.001 units distributed evenly between the niches (such that each niche required the same number of forward integration steps). The initial population abundances in all cases were random fractions of $\delta \cdot \rho_{\text{tot}}^{\text{max}}$, a dilution of the maximum biomass attainable by the population as per our model. Random numbers were drawn from a uniform distribution using Python 3's Random package.

Data, Materials, and Software Availability. There are no data underlying this work.

ACKNOWLEDGMENTS. This work was initiated at the Microbial ecology workshop that A.M. and T.H. participated in at the NSF-sponsored Kavli Institute of Theoretical Physics (NSF PHY-1748958). We are grateful for helpful discussions with numerous colleagues during the course of this work, including Milena Chakraverti-Wuerthwein, Martina dal Bello, Otto Cordero, Akshit Goyal, K.C. Huang, Seppe Kuehn, Pankaj Mehta, Fangzhou Xiao, Ben Good, Daniel Fisher, Ned Wingreen, and members of the Hwa lab. We also thank the two reviewers for their careful reading and many constructive comments that led to significant improvements in the content and presentation of the manuscript. A.V.N. and T.H. are supported by the Simons Foundation through the Principles of Microbial Ecosystems collaboration (Grant No. 542387) and by the NSF (MCB-2029574). A.M. is supported by the NIH under Award No. R35GM151211 and the NSF through the Center for Living Systems (Grant No. 2317138).

Author affiliations: [a]Department of Physics, University of California, San Diego, La Jolla, CA 92093-0319; and [b]Department of Physics, University of Chicago, Chicago, IL 60637

1. R. J. Lamont, H. Koo, G. Hajishengallis, The oral microbiota: Dynamic communities and host interactions. *Nat. Rev. Microbiol.* **16**, 745–759 (2018).
2. J. G. Caporaso *et al*., Moving pictures of the human microbiome. *Genome Biol.* **12**, 1–8 (2011).
3. G. K. Gerber, The dynamic microbiome. *FEBS Lett.* **588**, 4131–4139 (2014).
4. L. A. David *et al*., Host lifestyle affects human microbiota on daily timescales. *Genome Biol.* **15**, 1–15 (2014).
5. J. K. Jansson, K. S. Hofmockel, Soil microbiomes and climate change. *Nat. Rev. Microbiol.* **18**, 35–46 (2020).
6. N. V. Patin *et al*., Microbiome dynamics in a large artificial seawater aquarium. *Appl. Environ. Microbiol.* **84**, e00179-18 (2018).
7. P. L. Buttigieg *et al*., Marine microbes in 4d-using time series observation to assess the dynamics of the ocean microbiome and its links to ocean health. *Curr. Opin. Microbiol.* **43**, 169–185 (2018).
8. M. Gupta *et al*., A nutrient relay sustains subtropical ocean productivity. *Proc. Natl. Acad. Sci. U.S.A.* **119**, e2206504119 (2022).
9. B. H. Schlomann, R. Parthasarathy, Timescales of gut microbiome dynamics. *Curr. Opin. Microbiol.* **50**, 56–63 (2019).
10. S. M. Smith, M. Hanley, K. T. Killingbeck, Development of vegetation in dune slack wetlands of Cape Cod National Seashore (Massachusetts, USA). *Plant Ecol.* **194**, 243–256 (2008).
11. L. P. Braga, S. M. Soucy, D. E. Amgarten, A. M. Da Silva, J. C. Setubal, Bacterial diversification in the light of the interactions with phages: The genetic symbionts and their role in ecological speciation. *Front. Ecol. Evol.* **6**, 6 (2018).
12. J. E. Goldford *et al*., Emergent simplicity in microbial community assembly. *Science* **361**, 469–474 (2018).
13. M. Dal Bello, H. Lee, A. Goyal, J. Gore, Resource-diversity relationships in bacterial communities reflect the network structure of microbial metabolism. *Nat. Ecol. Evol.* **5**, 1424–1434 (2021).
14. K. Gowda, D. Ping, M. Mani, S. Kuehn, Genomic structure predicts metabolite dynamics in microbial communities. *Cell* **185**, 530–546 (2022).
15. C. Ratzke, J. Gore, Modifying and reacting to the environmental pH can drive bacterial interactions. *PLoS Biol.* **16**, e2004248 (2018).
16. K. Amarnath *et al*., Stress-induced metabolic exchanges between complementary bacterial types underly a dynamic mechanism of inter-species stress resistance. *Nat. Commun.* **14**, 3165 (2023).
17. K. Crocker *et al*., Environmentally dependent interactions shape patterns in gene content across natural microbiomes. *Nat. Microbiol.* **9**, 2022–2037 (2024).
18. P. Ghosh, J. Mondal, E. Ben-Jacob, H. Levine, Mechanically-driven phase separation in a growing bacterial colony. *Proc. Natl. Acad. Sci. U.S.A.* **112**, E2166–E2173 (2015).
19. S. Rebuffat, "Microcins from enterobacteria: On the edge between gram-positive bacteriocins and colicins" in *Prokaryotic Antimicrobial Peptides: From Genes to Applications*, D. Drider, S. Rebuffat, Eds. (Springer, New York, NY, 2011), pp. 333–349.
20. Z. Cao, M. G. Casabona, H. Kneuper, J. D. Chalmers, T. Palmer, The Type VII secretion system of *Staphylococcus aureus* secretes a nuclease toxin that targets competitor bacteria. *Nat. Microbiol.* **2**, 1–11 (2016).
21. L. García-Bayona, M. S. Guo, M. T. Laub, Contact-dependent killing by *Caulobacter crescentus* via cell surface-associated, glycine zipper proteins. *eLife* **6**, e24869 (2017).
22. R. M. May, *Stability and Complexity in Model Ecosystems* (Princeton University Press, 2019).
23. R. M. May, *Stability and Complexity in Model Ecosystems* (Princeton University Press, Princeton, NJ, 2001).
24. D. P. Newton, P. Y. Ho, K. C. Huang, Modulation of antibiotic effects on microbial communities by resource competition. *Nat. Commun.* **14**, 2398 (2023).
25. R. MacArthur, R. Levins, The limiting similarity, convergence, and divergence of coexisting species. *Am. Nat.* **101**, 377–385 (1967).
26. R. MacArthur, Species packing and competitive equilibrium for many species. *Theor. Popul. Biol.* **1**, 1–11 (1970).
27. D. Tilman, Resource competition between plankton algae: An experimental and theoretical approach. *Ecology* **58**, 338–348 (1977).
28. V. Volterra, Variations and fluctuations of the number of individuals in animal species living together. *ICES J. Mar. Sci.* **3**, 3–51 (1928).
29. P. Cai *et al*., Soil biofilms: Microbial interactions, challenges, and advanced techniques for ex-situ characterization. *Soil Ecol. Lett.* **1**, 85–93 (2019).
30. C. J. Wright *et al*., Microbial interactions in building of communities. *Mol. Oral Microbiol.* **28**, 83–101 (2013).
31. A. R. Pacheco, D. Segrè, A multidimensional perspective on microbial interactions. *FEMS Microbiol. Lett.* **366**, fnz125 (2019).
32. K. C. Abbott, K. Cuddington, A. Hastings, Transients in ecology: Stochasticity, management, and understanding. *Theor. Ecol.* **14**, 623–624 (2021).
33. S. Harrison, H. Cornell, K. A. Moore, Spatial niches and coexistence: Testing theory with tarweeds. *Ecology* **91**, 2141–2150 (2010).
34. N. Kronfeld-Schor, T. Dayan, Partitioning of time as an ecological resource. *Annu. Rev. Ecol. Evol. Syst.* **34**, 153–181 (2003).
35. H. S. Horn, The ecology of secondary succession. *Annu. Rev. Ecol. Evol. Syst.* **5**, 25–37 (1974).
36. M. S. Datta, E. Sliwerska, J. Gore, M. F. Polz, O. X. Cordero, Microbial interactions lead to rapid micro-scale successions on model marine particles. *Nat. Commun.* **7**, 1–7 (2016).
37. J. N. Butler, *Carbon Dioxide Equilibria and Their Applications* (Routledge, 2019).
38. S. Estrela, C. H. Trisos, S. P. Brown, From metabolism to ecology: Cross-feeding interactions shape the balance between polymicrobial conflict and mutualism. *Am. Nat.* **180**, 566–576 (2012).
39. B. R. Taylor *et al*., A metabolic sum rule dictates bacterial response to short-chain fatty acid stress. bioRxiv [Preprint] (2022). https://doi.org/10.1101/2022.08.31.506075 (Accessed 30 March 2025).
40. A. L. McCully *et al*., An *Escherichia coli* nitrogen starvation response is important for mutualistic coexistence with *Rhodopseudomonas palustris*. *Appl. Environ. Microbiol.* **84**, e00404-18 (2018).
41. S. Estrela *et al*., Functional attractors in microbial community assembly. *Cell Syst.* **13**, 29–42 (2022).
42. Y. Li *et al*., Hidden complexity of yeast adaptation under simple evolutionary conditions. *Curr. Biol.* **28**, 515–525 (2018).
43. P. Chesson, *Theoretical Ecology* (Oxford University Press, 2020), pp. 5–27.
44. R. MacArthur, R. Levins, Competition, habitat selection, and character displacement in a patchy environment. *Proc. Natl. Acad. Sci. U.S.A.* **51**, 1207 (1964).
45. B. Bloxham, H. Lee, J. Gore, Diauxic lags explain unexpected coexistence in multi-resource environments. *Mol. Syst. Biol.* **18**, e10630 (2022).
46. B. Bloxham, H. Lee, J. Gore, Biodiversity is enhanced by sequential resource utilization and environmental fluctuations via emergent temporal niches. *PLoS Comput. Biol.* **20**, e1012049 (2024).
47. A. Mahadevan, M. T. Pearce, D. S. Fisher, Spatiotemporal ecological chaos enables gradual evolutionary diversification without niches or tradeoffs. *eLife* **12**, e82734 (2023).

48. J. Huisman, F. J. Weissing, Biodiversity of plankton by species oscillations and chaos. *Nature* **402**, 407–410 (1999).
49. R. O. Moura, V. Calleja-Solanas, J. A. Langa, O. Godoy, A general framework for cycles in ecology. bioRxiv [Preprint] (2025). https://doi.org/10.1101/2025.01.13.632680 (Accessed 30 March 2025).
50. A. J. Lotka, "The growth of mixed populations: Two species competing for a common food supply" in *The Golden Age of Theoretical Ecology: 1923–1940*, F. M. Scudo, J. R. Ziegler, Eds. (Springer, 1978), pp. 274–286.
51. S. Suweis, F. Ferraro, C. Grilletta, S. Azaele, A. Maritan, Generalized Lotka–Volterra systems with time correlated stochastic interactions. *Phys. Rev. Lett.* **133**, 167101 (2024).
52. Y. Fridman, Z. Wang, S. Maslov, A. Goyal, Fine-scale diversity of microbial communities due to satellite niches in boom and bust environments. *PLoS Comput. Biol.* **18**, e1010244 (2022).
53. T. Gibbs, Y. Zhang, Z. R. Miller, J. P. O'Dwyer, Stability criteria for the consumption and exchange of essential resources. *PLoS Comput. Biol.* **18**, e1010521 (2022).
54. X. Wang, K. Xia, X. Yang, C. Tang, Growth strategy of microbes on mixed carbon sources. *Nat. Commun.* **10**, 1279 (2019).
55. Z. Wang *et al*., Complementary resource preferences spontaneously emerge in diauxic microbial communities. *Nat. Commun.* **12**, 6661 (2021).
56. W. M. Schaffer, M. Kot, Do strange attractors govern ecological systems? *BioScience* **35**, 342–350 (1985).
57. S. H. Strogatz, *Nonlinear Dynamics and Chaos: With Applications to Physics, Biology, Chemistry, and Engineering* (CRC Press, 2018).
58. F. M. Stewart, B. R. Levin, Partitioning of resources and the outcome of interspecific competition: A model and some general considerations. *Am. Nat.* **107**, 171–198 (1973).
59. K. B. Andersen, K. von Meyenburg, Are growth rates of *Escherichia coli* in batch cultures limited by respiration? *J. Bacteriol.* **144**, 114–123 (1980).
60. M. Manhart, B. V. Adkar, E. I. Shakhnovich, Trade-offs between microbial growth phases lead to frequency-dependent and non-transitive selection. *Proc. R. Soc. Lond. B, Biol. Sci.* **285**, 20172459 (2018).
61. D. Tilman, *Resource Competition and Community Structure* (Princeton University Press, 1982).
62. G. E. Hutchinson, The paradox of the plankton. *Am. Nat.* **95**, 137–145 (1961).
63. A. Erez, J. G. Lopez, B. G. Weiner, Y. Meir, N. S. Wingreen, Nutrient levels and trade-offs control diversity in a serial dilution ecosystem. *eLife* **9**, e57790 (2020).
64. T. Fukami, Historical contingency in community assembly: Integrating niches, species pools, and priority effects. *Annu. Rev. Ecol. Evol. Syst.* **46**, 1–23 (2015).
65. R. Kolter, D. A. Siegele, A. Tormo, The stationary phase of the bacterial life cycle. *Annu. Rev. Microbiol.* **47**, 855–874 (1993).
66. H. L. Smith, Bacterial competition in serial transfer culture. *Math. Biosci.* **229**, 149–159 (2011).
67. J. M. Navarro Llorens, Stationary phase in gram-negative bacteria. *FEMS Microbiol. Rev.* **34**, 476–495 (2010).
68. R. Marsland III, W. Cui, P. Mehta, A minimal model for microbial biodiversity can reproduce experimentally observed ecological patterns. *Sci. Rep.* **10**, 3308 (2020).
69. L. Wu *et al*., Assessing mechanisms for microbial taxa and community dynamics using process models. *mLife* **2**, 239–252 (2023).
70. J. Grilli, Macroecological laws describe variation and diversity in microbial communities. *Nat. Commun.* **11**, 4743 (2020).
71. S. Zaoli, J. Grilli, A macroecological description of alternative stable states reproduces intra-and inter-host variability of gut microbiome. *Sci. Adv.* **7**, eabj2882 (2021).
72. M. Shahin, B. Ji, P. D. Dixit, Embed,, Essential microbiome dynamics, a dimensionality reduction approach for longitudinal microbiome studies. *npj Syst. Biol. Appl.* **9**, 26 (2023).
73. P. Y. Ho, B. H. Good, K. C. Huang, Competition for fluctuating resources reproduces statistics of species abundance over time across wide-ranging microbiotas. *eLife* **11**, e75168 (2022).
74. R. D. Holt, Predation, apparent competition, and the structure of prey communities. *Theor. Popul. Biol.* **12**, 197–229 (1977).
75. G. Okpokwasili, C. Nweke, Microbial growth and substrate utilization kinetics. *Afr. J. Biotech.* **5**, 305–317 (2006).
76. K. B. Xavier, B. L. Bassler, LuxS quorum sensing: More than just a numbers game. *Curr. Opin. Microbiol.* **6**, 191–197 (2003).
77. K. Duan, C. Dammel, J. Stein, H. Rabin, M. G. Surette, Modulation of *Pseudomonas aeruginosa* gene expression by host microflora through interspecies communication. *Microbiol. Biotechnol.* **50**, 1477–1491 (2003).
78. A. W. Decho, R. S. Norman, P. T. Visscher, Quorum sensing in natural environments: Emerging views from microbial mats. *Trends Microbiol.* **18**, 73–80 (2010).
79. A. Vendeville, K. Winzer, K. Heurlier, C. M. Tang, K. R. Hardie, Making 'sense' of metabolism: Autoinducer-2, LuxS and pathogenic bacteria. *Nat. Rev. Microbiol.* **3**, 383–396 (2005).
80. S. C. De Keersmaecker, K. Sonck, J. Vanderleyden, Let LuxS speak up in AI-2 signaling. *Trends Microbiol.* **14**, 114–119 (2006).
81. W. R. Galloway, J. T. Hodgkinson, S. D. Bowden, M. Welch, D. R. Spring, Quorum sensing in gram-negative bacteria: Small-molecule modulation of AHL and AI-2 quorum sensing pathways. *Chem. Rev.* **111**, 28–67 (2011).
82. I. Janausch, E. Zientz, Q. Tran, A. Kröger, G. Unden, C4-dicarboxylate carriers and sensors in bacteria. *Biochim. Biophys. Acta, Bioenergetics* **1553**, 39–56 (2002).
83. S. Eriksson, R. Hurme, M. Rhen, Low-temperature sensors in bacteria. *Philos. Trans. R. Soc. Lond. Ser. B, Biol. Sci.* **357**, 887–893 (2002).
84. G. A. O'Toole, G. C. Wong, Sensational biofilms: Surface sensing in bacteria. *Curr. Opin. Microbiol.* **30**, 139–146 (2016).
85. T. A. Krulwich, G. Sachs, E. Padan, Molecular aspects of bacterial pH sensing and homeostasis. *Nat. Rev. Microbiol.* **9**, 330–343 (2011).
86. J. Barandica *et al*., A mathematical model for toxin accumulation by killer yeasts based on the yeast population growth. *J. Appl. Microbiol.* **86**, 805–811 (1999).
87. H. M. Doekes, R. J. De Boer, R. Hermsen, Toxin production spontaneously becomes regulated by local cell density in evolving bacterial populations. *PLoS Comput. Biol.* **15**, e1007333 (2019).
88. J. P. Grover, J. T. Scott, D. L. Roelke, B. W. Brooks, Dynamics of nitrogen-fixing cyanobacteria with heterocysts: A stoichiometric model. *Mar. Freshw. Res.* **71**, 644–658 (2019).
89. R. Niehus, N. M. Oliveira, A. Li, A. G. Fletcher, K. R. Foster, The evolution of strategy in bacterial warfare via the regulation of bacteriocins and antibiotics. *eLife* **10**, e69756 (2021).
90. D. Gonzalez, D. A. Mavridou, Making the best of aggression: The many dimensions of bacterial toxin regulation. *Trends Microbiol.* **27**, 897–905 (2019).
91. A. Maldonado-Barragán, S. A. West, The cost and benefit of quorum sensing-controlled bacteriocin production in *Lactobacillus plantarum*. *J. Evol. Biol.* **33**, 101–111 (2020).